CCS Chemistry

RESEARCH ARTICLE

Received: Nov. 11, 2019 | Accepted: Dec. 23, 2019

Pressing-Induced Caking: A General Strategy to Scale-Span Molecular Self-Assembly

Hongjun Jin[1†], Mengqi Xie[1†], Wenkai Wang[1], Lingxiang Jiang[2], Wenying Chang[3], Yue Sun[4], Limin Xu[1], Shihao Zang[1], Jianbin Huang[1], Yun Yan[1*] & Lei Jiang[4,5]

[1]Beijing National Laboratory for Molecular Sciences (BNLMS), College of Chemistry and Molecular Engineering, Peking University, Beijing 100871 (China), [2]College of Chemistry and Materials Science, Jinan University, Guangzhou 510632 (China), [3]Key Laboratory of Polymer Chemistry and Physics of Ministry of Education, College of Chemistry, Peking University, Beijing 100871 (China), [4]Key Laboratory of Bio-Inspired Smart Interfacial Science and Technology of Ministry of Education, School of Chemistry, Beihang University, Beijing 100191 (China), [5]CAS Key Laboratory of Bio-inspired Materials and Interfacial Science, CAS Center for Excellence in Nanoscience, Technical Institute of Physics and Chemistry, Chinese Academy of Sciences, Beijing 100190 (China)

*Corresponding author: yunyan@pku.edu.cn; †H. Jin and M. Xie contributed equally to this work.

Cite this: *CCS Chem*. **2020**, *2*, 98–106

General strategies leading to scale-span molecular self-assembly are of crucial importance in creating bulk supramolecular materials. Here, we report that under mechanical pressure, caking of the precipitated molecular self-assemblies led to bulk supramolecular films. Massive fabrication of supramolecular films became possible by employing a simple household noodle machine. The film could be endowed to acquire diversified functions by depositing various functional ingredients via coprecipitation. We expect that our current work opens up a new paradigm leading to large-scale functional solid molecular self-assembled materials.

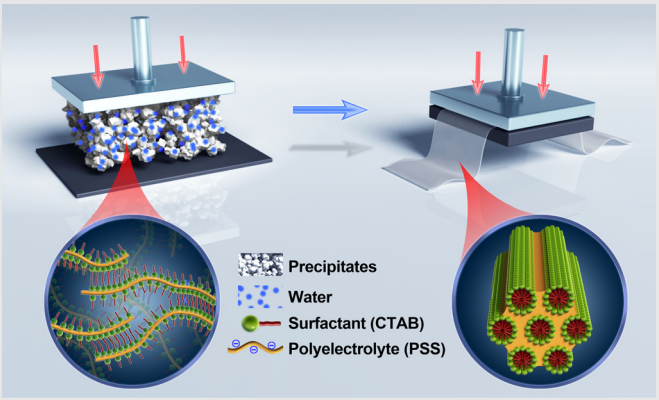

Keywords: **self-assembly, pressing, film, large scale**

Introduction

Molecular self-assembly represents a practical bottom-up process to create structural materials with emergent functionalities.[1–4] Typically, they are prepared in solutions in the form of suspensions,[5,6] which have rare applications in places where solid materials of large scales are required. Since solid materials are employed extensively in fields ranging from military to everyday life, scale-span molecular self-assembly is highly desirable for the achievement of solid supramolecular materials. However, so far, except for various hydrogel,[7–11] Layer-by-Layer (LBL) films,[12,13] casting-films,[14] or polymeric composite materials,[15–17] few molecular self-assembly could lead to other scale-span bulk solid structures.[18,19]

In contrast, nature is very good at creating scale-span behaviors. The most common example is the caking of powder materials, such as milk powder,[20] which is a process of aggregation of small crystalline particles into a large one.[20,21] One of the main reasons for caking is the moisture-triggered rearrangement of molecules or ions to form bridges between the individual particles.[21,22]

DOI: 10.31635/ccschem.020.201900088
CCS Chem. **2020**, *2*, 98–106

Accordingly, the formation of giant cakes reduces the interfaces between particles, thereby, assuming much lower energy, which triggers a spontaneous caking process.[22] Powders composed of irregular or polydispersed crystalline particles undergo caking readily owing to the sizeable interparticle contact areas.[23] This inspired the concept that caking might also occur in the precipitated molecular self-assembling system, as the self-assembled domains are similar to micro-crystalline structures, predicted to act as "crystalline seeds" in the process of caking. Compared with conventional powder materials containing small crystalline particles, the particles in the precipitated molecular self-assemblies likely have a strong tendency to merge, owing to the presence of non-covalent interactions between the molecules on the edge of neighboring particles. Therefore, we proposed that if the particles in the precipitated molecular self-assembling system were condensed enough, they would merge into a bulk material via rearrangement of molecules. Herein, we report that under mechanical pressure, the caking of condensed precipitates containing ordered molecular domain indeed leads to scale-span molecular self-assembly, which transforms the amorphous precipitates into an entire transparent supramolecular film. Due to the well-known fact that the oppositely charged polyelectrolyte (PE)-surfactant systems form precipitates containing ordered surfactant domains,[24] we started this research with PE-surfactant precipitates and subsequently, fabricated them into a bulk film. Our research revealed that the disordered small surfactant domains in the precipitates might have transformed into liquid crystalline mesophases under mechanical pressure, which reduced the domain boundaries to form the bulk film. The crystalline mesophases rendered the film with excellent birefringence, and the alternatively arranged hydrophobic/hydrophilic domains made it possible to dope various functional components facilely through coprecipitation in water, regardless of their hydrophobicity and afforded the film with an open platform for diversified functions. In particular, biomolecules, such as enzymes, were able to sustain activity in the film. It is a general method to develop scale-span bulk supramolecular films by pressing any combination of oppositely charged PE and surfactant. The simplicity of their fabrication, their availability from both renewable and commercial resources, their judicious functional modality, and the possibility of industrial-scale production, bode well for future applications.

Experimental Methods

Materials and chemicals

Cetyl trimethyl ammonium bromide (CTAB) and 1-butyl-3-methyl imidazole acetate ([BMIm]Ac) were purchased from Aladdin Industrial Corporation (Beijing, China) and were used as received. Sodium polystyrene sulfonate (PSS; M_w ~ 70,000) was purchased from Sigma-Aldrich Corporation (Shanghai, China). All other reagents used were of analytical reagents (AR) grade. The aqueous solutions were prepared by using Milli-Q water of 18 MΩ.

Precipitate and film formation

To an aqueous solution of PSS, an aqueous solution of CTAB was added, reaching final concentrations of 20 mM for the negative charges of PSS and positive charges of CTAB. The white precipitates formed were separated by centrifugation at 5000 rpm. Then the collected precipitates were pressed by fingers or a noodle machine to form transparent plastic films. For films generated in the mixed solvent of water–ionic liquid, the same procedure was carried out using 9:1 mixed H_2O and [BMIm]Ac (volume ratio). Doping of functional molecules was performed by varying added dopants in the aqueous solution of CTAB or PSS before mixing; these dopants were coprecipitated in the process of mixing the two oppositely charged solutions. The same pressing procedure as the PSS/CTAB film was adopted to obtain functional films.

Mechanical tests

The mechanical properties of the plastic films were tested using a WDW3020 electronic universal testing machine at room temperature and 50% relative humidity. These include graphs obtained from stress–strain curves, tensile strength parameters, maximum strains, and Young's moduli, and stress–strain data were gathered with a strain rate of 1 mm/min. The thicknesses of the films ranged from 20 to 400 μm. Dumbbell-shaped samples were utilized to conduct all mechanical tests shown as a model in Supporting Information Figure S15. Samples undergoing different remolding cycles of the same original film were used to measure the outstanding juvenescence ability of the materials.

Characterizations of the films

We carried out elemental analyses of the films using energy-dispersive spectroscopy (EDS) measurement with a Hitachi S4800 microscope (Shanghai, China) at an acceleration voltage of 7 kV (Supporting Information Table S2) and Vario EL elemental analyzer (Elementar Analysensysteme GmbH, Langenselbold, Germany). We performed X-ray diffraction (XRD) measurements using a Rigaku D/max-2400 diffractometer (Tokyo, Japan) with Cu Kα radiation. Two-dimensional (2D) small-angle X-ray scattering (2D-SAXS; Qingdao Jiuyi Graphite Co., Ltd., Shandong, China) patterns of the films, and the powders were recorded by a Ganesha SAXS system with a 2D detector. Polarized microscopy was obtained with an

DOI: 10.31635/ccschem.020.201900088
CCS Chem. **2020**, *2*, 98–106

LV100N polarizing microscope (Nikon Co., Irving, CA) in ambient environmental conditions (room temperature = 20–25 °C; pressure = 1 atm; humidity = 50–60%). Samples were photographed with θ ranging from 0° to 359°, where θ is the angle between the analyzer and the alignment direction of the sample.

Results and Discussion

We demonstrate the strategy of scale-span molecular self-assembly using the pressing-induced caking of the precipitates formed by the oppositely charged PE-surfactant pair of sodium PSS and CTAB. It is well-known that upon mixing the two aqueous solutions at charge balancing ratio, they form white precipitates, which could be cast into thin films from organic solution after washing and drying several times to remove inorganic salts.[25] Our study showed that the PSS–CTAB precipitates could be transformed directly into a large transparent film after pressing the precipitates with a mild mechanical pressure of ~5 MPa, as illustrated in Figure 1a. All the tested combinations of the oppositely charged polyelectrolytes and surfactants in this study could serve a purpose (see Supporting Information Table S1 and Figures S1–S3).

Contrary to the white precipitates that are dark under polarized optical microscopy (POM) (Figure 2a and b), the self-supporting transparent film displays strong birefringence (Figure 2c–e). Figure 2f shows that the XRD pattern of the original precipitates has weak diffraction in the low-angle region. The distance corresponding to this diffraction is 4.3 nm, which is nearly twice as long as the extending length of the CTAB molecule (2.2 nm), confirming that there are ordered surfactant domains in the precipitates (illustrated as an inset in Figure 2f). However, the diffraction peak for the film is sharpened extensively and intensified, indicating an increase in the size of the surfactant domains.[26] According to the Scherrer equation,[27] the average domain size in the precipitates and the consequent film are ~40 nm and 400 nm, respectively. The large size of 400 nm is comparable to visible light, which is the reason why the film displayed birefringence.[28] 2D-SAXS measurements displayed concentric rings both for the original precipitates and for the film (Figure 1b), indicating that the large surfactant domains in the film, similar to the small ones present in the precipitates, are randomly oriented.

Notably, the sharpened and intensified diffraction peak of the film (Figure 2f) is followed by two extra weak diffractions. The three diffractions acquired a spacing ratio of $1:\sqrt{3}:\sqrt{4}$, corresponding to (100), (110), and (200) Miller Indices of a 2D hexagonal mesostructure, respectively.[29–31] The corresponding lattice parameter, a, is 4.9 nm, where $a = 4\pi\frac{\sqrt{h^2+k^2+hk}}{\sqrt{3}q_{hkl}}$.[32] This means that under mechanical pressure, the CTAB molecules, which are bonded electrostatically to the PSS chains, rearranged into wormlike micelles, and packed further into hexagonal phases[33] (inset in Figure 2f).

The role of the mechanical pressure was to condense the precipitates. Figure 3a shows that the application of small pressure only led to condensed precipitates, as

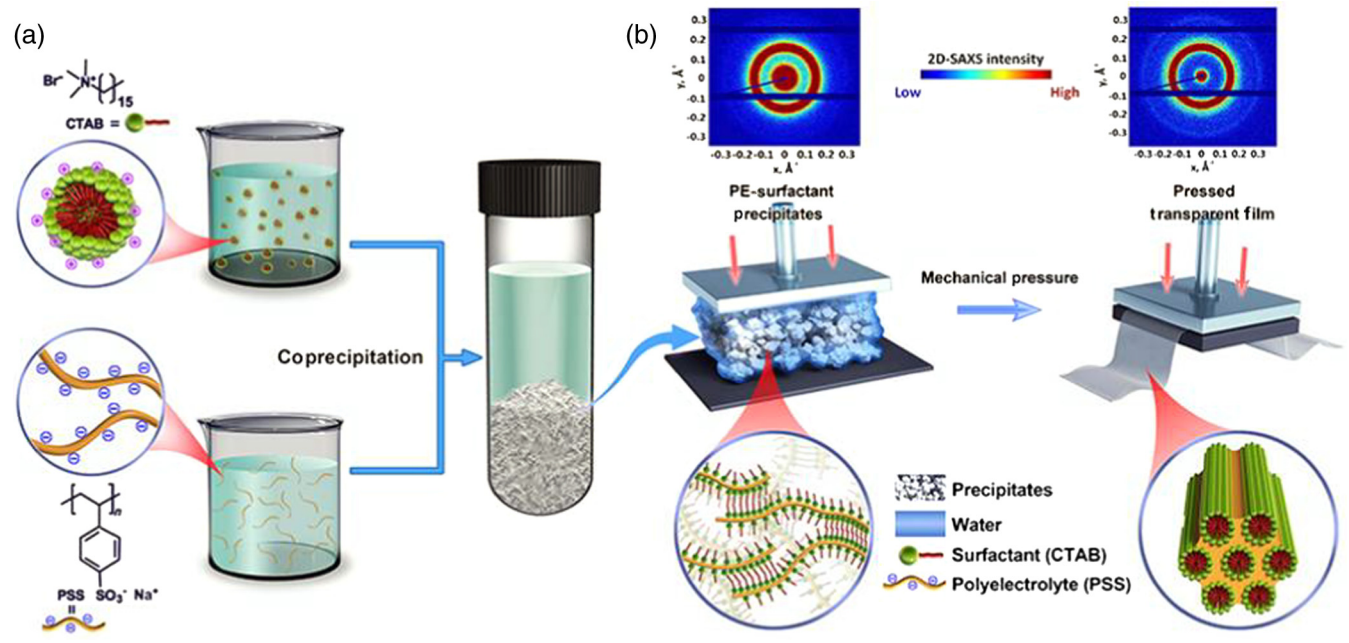

Figure 1 | *(a) Press-induced transparent supramolecular films from precipitated polyelectrolyte–surfactant complexes, illustrated with the sodium PSS and CTAB system. (b) 2D-SAXS for the precipitates and the film, respectively.*

DOI: 10.31635/ccschem.020.201900088
CCS Chem. **2020**, *2*, 98–106

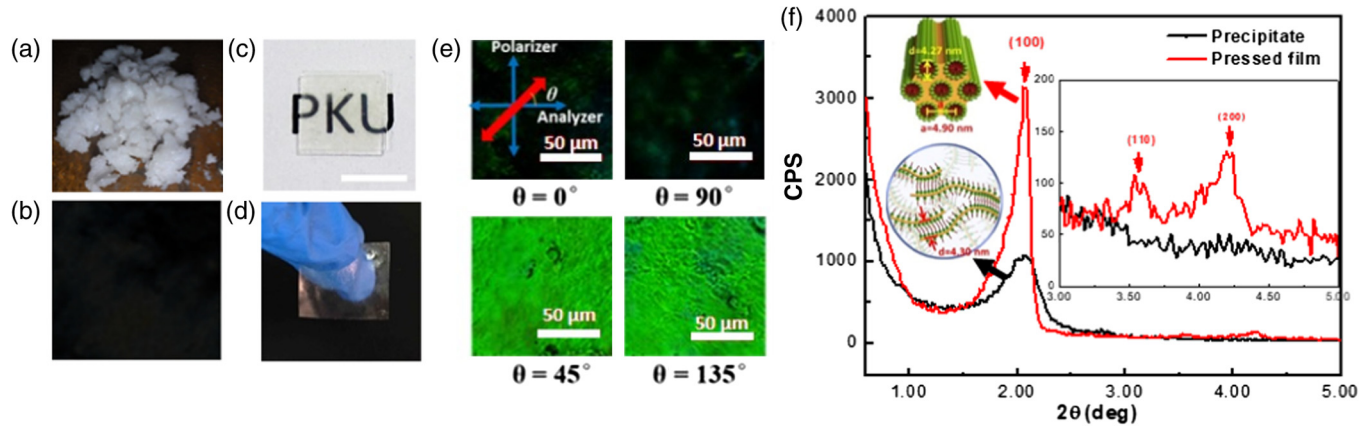

Figure 2 | *(a, b) The precipitates of sodium PSS/CTAB under polarizer; (c, d) the film obtained by pressing the precipitate in (a). The scale bar in (c) is 1 cm. (e) The birefringence of the fabricated film. (f) XRD pattern of the precipitate and the film, respectively. The insets show the molecular arrangement in the precipitate and the film, respectively.*

reflected by the diffraction intensities being proportional to the pressure (inset in Figure 3a). However, the size of the ordered molecular domain did not increase appreciably since the width of the diffraction peak remained almost unchanged. Water is very crucial in the rearrangement of the molecules and the film formation. Our thermogravimetric (TGA) analysis suggested that there was 9% water in the precipitates (Figure 3b). When these water molecules were removed by freeze-drying with subsequent pressure application, it did not lead to transparent film formation (Figure 3c), and the X-ray diffraction intensity of the resultant white cake remained the same as the original precipitate (Supporting Information Figure S4). However, upon loading with a drop of water, the white cake spontaneously transformed into a transparent film within 15 min (Figure 3c), accompanied by the occurrence of birefringence (Figure 3c). The XRD pattern of the directly pressed film and the water-triggered film were identical (Figure 3d), and TGA measurements revealed that the films had the exact amount of water as the precipitates (Figure 3b). This confirmed that a caking process, as illustrated in Figure 3e, had occurred in the condensed precipitates, and because of the presence of strong van der Waals attraction between the surfactant chains, the small surfactant domains rearranged to form long wormlike micelles, which further, tightly packed into hexagonal mesophases.

Also, the bridging ability of PSS chains between these randomly oriented surfactant domains of CTAB is very crucial. As PSS was replaced by small anionic molecule such as the anionic surfactant, sodium dodecylbenzene sulfide (SDBS), application of mechanical pressure failed to lead to a self-supporting film (Supporting Information Figure S5). Nonetheless, almost any combination of oppositely charged PE and surfactant resulted in self-supporting transparent films (Supporting Information Table S1 and Figures S1–S3), but the lattice structure in the mesophase might vary widely with different combinations of PE-surfactant, similar to the casted PE-surfactant films.[25,32,34,35] We observed both hexagonal phases (Supporting Information Figure S6) and lamellar phases (Supporting Information Figure S7) for various tested systems. Therefore, we inferred that the film formation is indeed highly analogous to the caking process that occurs naturally in powder materials.

The caking-facilitated scale-span molecular self-assembly allows the fabrication of large-scale birefringent film materials. By loading the kneaded fresh precipitates, just as loading a kneaded dough to a household noodle machine, a massive production of the birefringent film was possible (Figure 4a). Figure 4b shows a 20 cm × 30 cm film, which could be produced in rolls (Figure 4c). Figure 4d is the birefringence of the large film in between two 20 cm × 20 cm polarizers. Furthermore, this new principle of scale-span supramolecular films allowed manipulation of the mechanical property and the function of the film to occur readily. For instance, if the solvent water was replaced with the mixed solvent of water and ionic liquid, the mechanical strength and the brittleness of the film could be improved. Figure 4e shows that without employing the ionic liquid, 1-butyl-3-methyl imidazole acetate ([BMIm]Ac), the film could endure maximum stress of ~0.6 MPa with a strain of ~10%. In contrast, replacement of water by a mixture of water/[BMIm]Ac at a volume ratio of 9:1, the maximum stress was enhanced to 1.0 MPa, and the strain attained was as high as 75%. Figure 4f shows that the film generated from aqueous precipitates becomes fragile due to loss of water at a humidity below 30%, whereas that produced from water–ionic liquid mixtures are flexible under the same condition, and thus, could be bent and folded freely just like plastics. TGA and proton

DOI: 10.31635/ccschem.020.201900088
CCS Chem. **2020**, *2*, 98–106

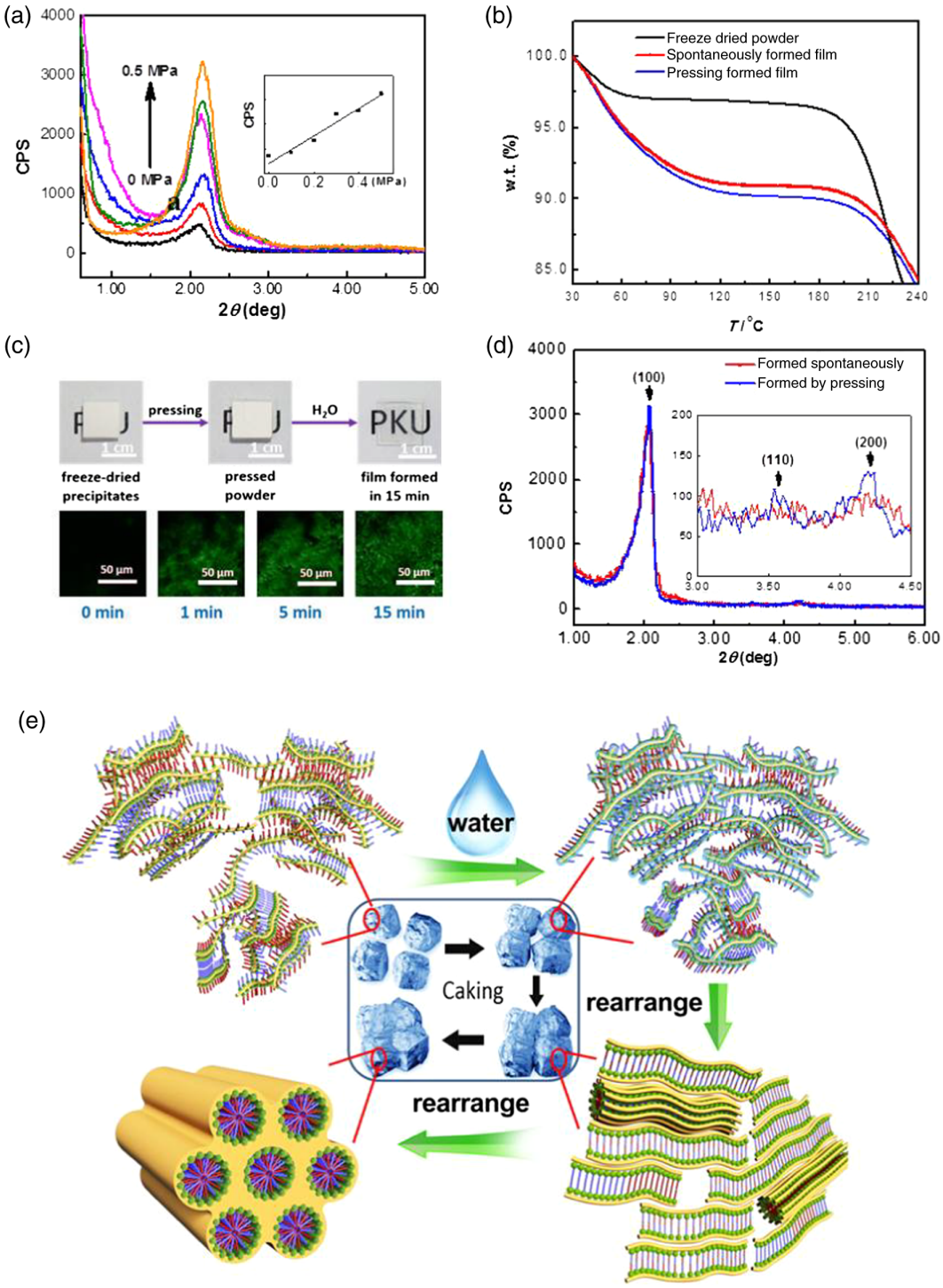

Figure 3 | *(a) Variation of the XRD intensity as increasing mechanical pressure; (b) TGA curves for the film, the freeze-dried precipitate, and the water-treated pressed precipitate. (c) Variation of the birefringence with time for water-treated precipitate. (d) Comparison of the XRD patterns for the films obtained by pressing and water-enabled spontaneous formation. (e) Illustration of water-facilitated rearrangement of the molecules in the caking process of the sodium PSS/CTAB precipitate.*

nuclear magnetic resonance (^{1}H NMR) measurements revealed that the water molecules in the film had been replaced by the nonevaporating ionic liquid molecules (Supporting Information Figures S8 and S9).

Finally, the caking-facilitated film has many advantages over casting films. First of all, the entire aqueous process and the presence of water allowed the preservation of the activity of enzymes in the film. As a demonstration,

DOI: 10.31635/ccschem.020.201900088
CCS Chem. **2020**, *2*, 98–106

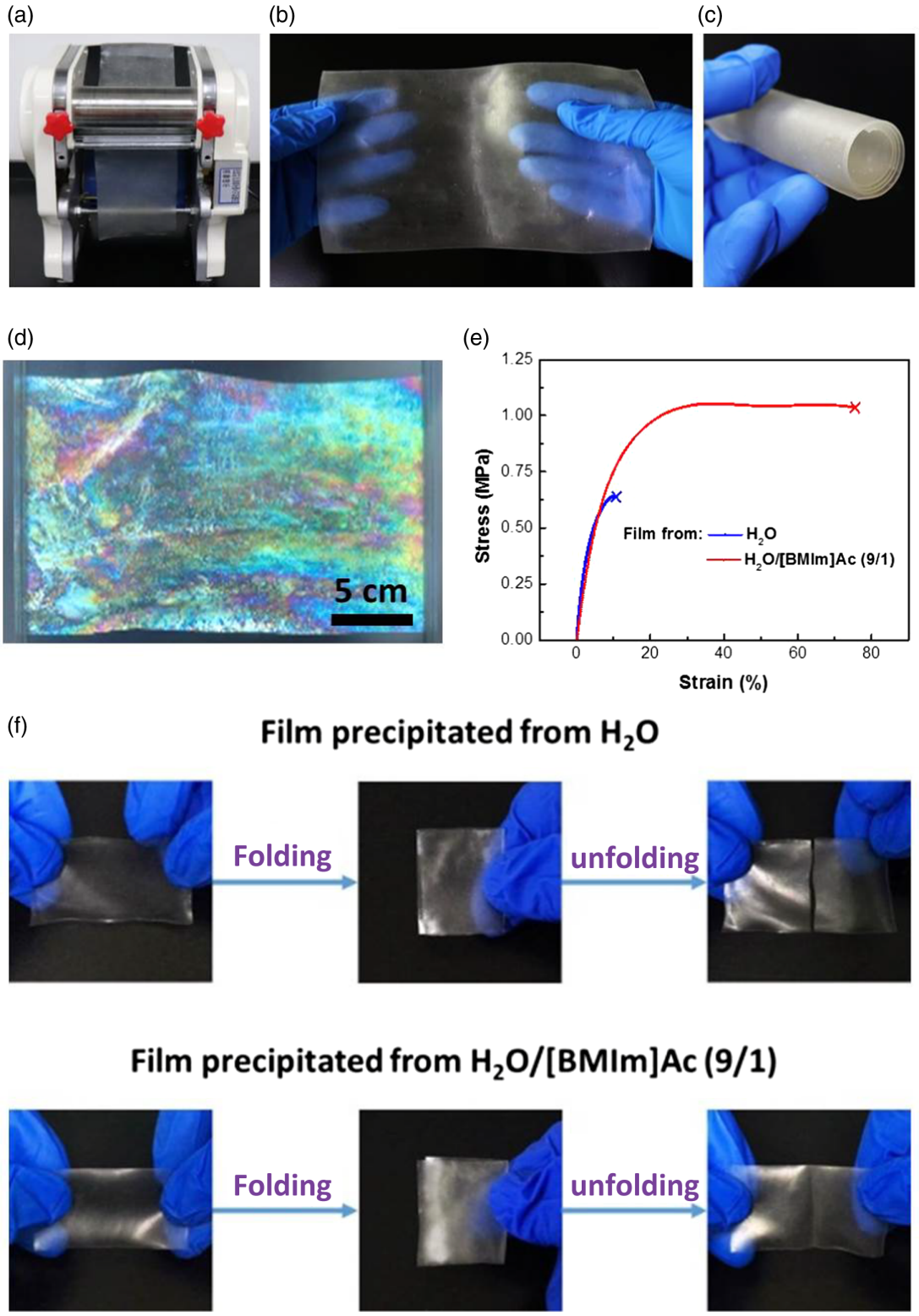

Figure 4 | *(a) Massive fabrication of a sodium PSS/CTAB film using a household noodle machine; (b) a 20 cm × 30 cm PSS/CTAB film generated with the noodle machine; (c) the film in (b) can be rolled. (d) The birefringence of the large-scale PSS/CTAB film observed in-between two vertically aligned 30 cm × 30 cm polarizers. (e) Comparison of the brittleness of the film prepared from aqueous precipitates and water–ionic liquid mixed solvent. The ionic liquid is 1-butyl-3-methyl imidazole acetate ([BMIm]Ac) used in the film-fabrication reaction and the volume ratio of H_2O/[BMIm]Ac = 9/1. (f) Comparison of the mechanical property of the films made from water and that from the mixed solvent of H_2O/[BMIm]Ac = 9/1.*

DOI: 10.31635/ccschem.020.201900088
CCS Chem. **2020**, *2*, 98–106

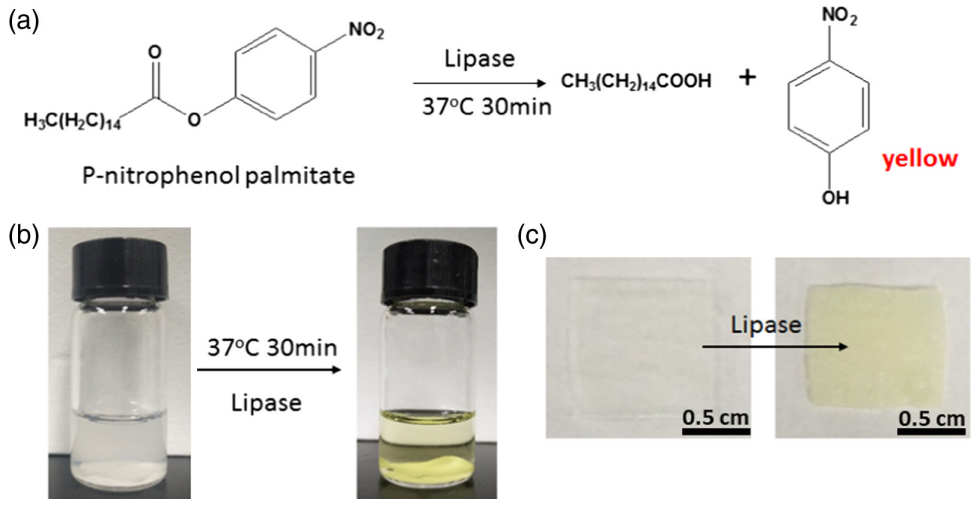

Figure 5 | *Lipase testing film by doping the hydrophobic testing kit p-nitrophenol palmitate into the sodium PSS/CTAB film. (a) The lipase-triggered hydrolysis reaction of p-nitrophenol palmitate. (b) Photographs, showing the color change of the lipase solution (in phosphate buffer) in the presence of a PSS/CTAB film doped with p-nitrophenol. The lipase reaction was set at 37 °C. (c) Photographs, showing the color change of the film after the lipase-triggered reaction occurring in the buffer.*

we have shown in Figure 5 that the p-nitrophenol palmitate (PNPP)-doped film was permeable to lipase and maintained its activity: The PNPP-doped film was transparent initially but turned yellow when incubated in lipase buffer, as a result of hydrolysis of the colorless PNPP into yellow p-nitrophenol.[36] This indicated that the lipase enzyme was able to diffuse into the film and retained its catalytic activity. Since an abnormally high level of lipase features a condition known as acute pancreatitis,[37] which imposes a severe threat to people's lives, the PNPP-doped film is promising for easy detection of the degree of lipase activity in a clinical setting.

Secondly, the presence of orderly arranged hydrophobic/hydrophilic domains allows the doping of various functional components into a film, regardless of their hydrophobicity, which opens up a material protocol

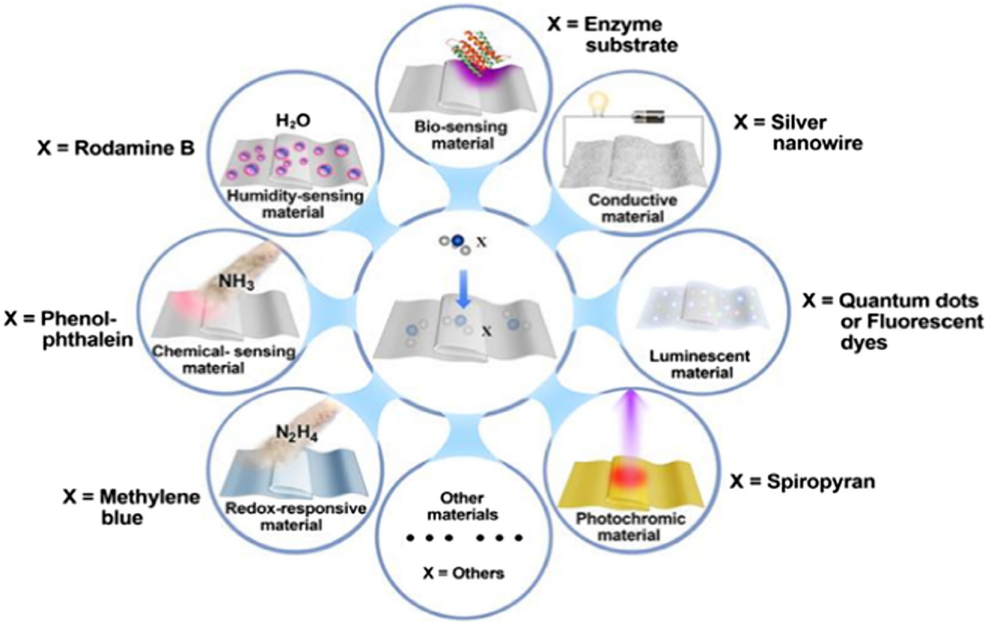

Figure 6 | *Illustration of the multifunctionality of the sodium PSS/CTAB film by doping with different functional agents.*

DOI: 10.31635/ccschem.020.201900088
CCS Chem. **2020**, *2*, 98–106

leading to multifunctional platforms. Almost all functional molecules, ranging from nanoparticles to polymers, irrespective of their hydrophobicity, could be doped into the film by coprecipitation, rendering it an open platform toward functional diversity. As a conceptual description, Figure 6 illustrates that the film could be fabricated into humidity-responsive, biosensing, conductive, luminescent, photochromic, chemical-sensing, and redox-responsive materials, to name a few. Extended data for these examples could be found in Supporting Information Figures S10–S14.

Conclusion

We report a general strategy of pressing-facilitated scale-scan molecular self-assembly, initiated by generation of precipitates containing self-assembled nanostructures. Mechanical pressure application condensed the particles present in the precipitates. Accessibility of physically adsorbed water facilitates the surfactant chains toward rearrangement, owing to the strong van der Waals attraction between the surfactant chains, and leads to the formation of large surfactant mesophases. These mesophases are connected further by the PE chains to form a bulk film. This process is highly analogous to the caking of powder materials in nature, which is an energy-favorable process. We have shown in our present study that any combination of oppositely charged PE and surfactant displays such thermodynamically feasible behavior. We have, thus, developed a general method leading to scale-span bulk molecular self-assembly, which holds the promise of building massive advanced supramolecular materials.

Supporting Information

Supporting Information is available.

Conflict of Interest

The authors declare no conflicts.

Funding Information

This work was supported financially by the National Natural Science Foundation of China (NSFC 91856120, 21573011, and 21633002).

Acknowledgments

The authors acknowledge Professor Steve Granick and Benzhong Tang for their helpful suggestions and discussions, and Professor Jianling Zhang from the Beijing Chemistry Institute, the Chinese Academy of Science for the generous offering of ionic liquids.

References

1. Ward, M. D.; Raithby, P. R. Functional Behaviour From Controlled Self-Assembly: Challenges and Prospects. *Chem. Soc. Rev.* **2013**, *42*, 1619–1636.
2. Jones, M. R.; Mirkin, C. A. Self-Assembly Gets New Direction. *Nature* **2012**, *491*, 42–43.
3. Kong, E. H.; Ding, B. J.; Li, M. H.; Li, Y. C.; Wu, Z. G.; Zhang, L.; Liu, F. K.; Shan, J. F.; Zhang, X. J.; Qin, C. M.; Xu, G. S.; Wang, H. Q.; Gong, X. Z.; Gan, K. F.; Wang, M.; Feng, J. Q. Density Modification in the Scrape-Off-Layer During LHW Coupling at EAST. *Plasma. Phys. Contr. F.* **2014**, *56*, 075016.
4. Faul, C. F. J. Ionic Self-Assembly for Functional Hierarchical Nanostructured Materials. *Accounts Chem. Res.* **2014**, *47*, 3428–3438.
5. Gorl, D.; Zhang, X.; Stepanenko, V.; Wurthner, F. Supramolecular Block Copolymers by Kinetically Controlled Co-Self-Assembly of Planar and Core-Twisted Perylene Bisimides. *Nat. Commun.* **2015**, *6*, 7009.
6. Zhang, X.; Wang, C. Supramolecular Amphiphiles. *Chem. Soc. Rev.* **2011**, *40*, 94–101.
7. Han, L.; Yan, L. W.; Wang, M. H.; Wang, K. F.; Fang, L. M.; Zhou, J.; Fang, J.; Ren, F. Z.; Lu, X. Transparent, Adhesive, and Conductive Hydrogel for Soft Bioelectronics Based on Light-Transmitting Polydopamine-Doped Polypyrrole Nanofibrils. *Chem. Mater.* **2018**, *30*, 5561–5572.
8. Ye, Y. N.; Frauenlob, M.; Wang, L.; Tsuda, M.; Sun, T. L.; Cui, K. P.; Takahashi, R.; Zhang, H. J.; Nakajima, T.; Nonoyama, T.; Kurokawa, T.; Tanaka, S.; Gong, J. P. Tough and Self-Recoverable Thin Hydrogel Membranes for Biological Applications. *Adv. Funct. Mater.* **2018**, *28*, 1801489.
9. Nonoyama, T.; Gong, J. P. Double-Network Hydrogel and Its Potential Biomedical Application: A Review. *P I Mech. Eng. H.* **2015**, *229*, 853–863.
10. Zhao, T. H.; Han, J. L.; Jin, X.; Liu, Y.; Liu, M. H.; Duan, P. F. Enhanced Circularly Polarized Luminescence from Reorganized Chiral Emitters on the Skeleton of a Zeolitic Imidazolate Framework. *Angew. Chem.-Int. Ed.* **2019**, *58*, 4978–4982.
11. Zhao, Z. G.; Li, C. X.; Dong, Z. C.; Yang, Y. C.; Zhang, L. H.; Zhuo, S. Y.; Zhou, X. T.; Xu, Y. C.; Jiang, L.; Liu, M. J. Adaptive Superamphiphilic Organohydrogels with Reconfigurable Surface Topography for Programming Unidirectional Liquid Transport. *Adv. Funct. Mater.* **2019**, *29*, 1807858.
12. Wang, X.; Wang, Y.; Bi, S.; Wang, Y. G.; Chen, X. G.; Qiu, L. Y.; Sun, J. Q. Optically Transparent Antibacterial Films Capable of Healing Multiple Scratches. *Adv. Funct. Mater.* **2014**, *24*, 403–411.
13. Wang, Y.; Li, T. Q.; Li, S. H.; Guo, R. B.; Sun, J. Q. Healable and Optically Transparent Polymeric Films Capable of Being Erased on Demand. *ACS Appl. Mater. Inter.* **2015**, *7*, 13597–13603.
14. Burnworth, M.; Tang, L. M.; Kumpfer, J. R.; Duncan, A. J.; Beyer, F. L.; Fiore, G. L.; Rowan, S. J.; Weder, C. Optically Healable Supramolecular Polymers. *Nature* **2011**, *472*, 334–U230.
15. An, N.; Wang, X. H.; Li, Y. X.; Zhang, L.; Lu, Z. Y.; Sun, J. Q. Healable and Mechanically Super-Strong Polymeric

DOI: 10.31635/ccschem.020.201900088
CCS Chem. **2020**, *2*, 98–106

Composites Derived from Hydrogen-Bonded Polymeric Complexes *Adv. Mater.* **2019**, *31*, 1904882.
16. Wang, Y.; Liu, X. K.; Li, S. H.; Li, T. Q.; Song, Y.; Li, Z. D.; Zhang, W. K.; Sun, J. Q. Transparent, Healable Elastomers with High Mechanical Strength and Elasticity Derived from Hydrogen-Bonded Polymer Complexes. *ACS Appl. Mater. Inter.* **2017**, *9*, 29120–29129.
17. Lu, X. Y.; Luo, Y. C.; Li, Y. X.; Bao, C. Y.; Wang, X. H.; An, N.; Wang, G. B.; Sun, J. Q. Polymeric Complex Nanoparticles Enable the Fabrication of Mechanically Superstrong and Recyclable Poly(aryl ether sulfone)-based Polymer Composites. *CCS Chem.* **2019**, *1*, 524–532.
18. Yamada, N.; Komatsu, T.; Yoshinaga, H.; Yoshizawa, K.; Edo, S.; Kunitake, M. Self-Supporting Elastic Film Without Covalent Linkages as a Hierarchically Integrated Beta-Sheet Assembly. *Angew. Chem.-Int. Ed.* **2003**, *42*, 5496–5499.
19. Lunn, D. J.; Gould, O. E. C.; Whittell, G. R.; Armstrong, D. P.; Mineart, K. P.; Winnik, M. A.; Spontak, R. J.; Pringle, P. G.; Manners, I. Microfibres and Macroscopic Films from the Coordination-Driven Hierarchical Self-Assembly of Cylindrical Micelles. *Nat. Commun.* **2016**, *7*, 12371.
20. Aguilera, J. M.; Delvalle, J. M.; Karel, M. Caking Phenomena in Amorphous Food Powders. *Trends Food Sci. Tech.* **1995**, *6*, 224–224.
21. Zafar, U.; Vivacqua, V.; Calvert, G.; Ghadiri, M.; Cleaver, J. A. S. A Review of Bulk Powder Caking. *Powder Technol.* **2017**, *313*, 389–401.
22. Lipasek, R. A.; Ortiz, J. C.; Taylor, L. S.; Mauer, L. J. Effects of Anticaking Agents and Storage Conditions on the Moisture Sorption, Caking, and Flowability of Deliquescent Ingredients. *Food Res. Int.* **2012**, *45*, 369–380.
23. Carpin, M.; Bertelsen, H.; Bech, J. K.; Jeantet, R.; Risbo, J.; Schuck, P. Caking of Lactose: A Critical Review. *Trends Food Sci. Tech.* **2016**, *53*, 1–12.
24. Trabelsi, S.; Albouy, P. A.; Imperor-Clerc, M.; Guillot, S.; Langevin, D. X-ray Diffraction Study of the Structure of Carboxymethylcellulose-Cationic Surfactant Complexes. *Chemphyschem* **2007**, *8*, 2379–2385.
25. Antonietti, M.; Conrad, J.; Thunemann, A. Polyelectrolyte-Surfactant Complexes–a New-Type of Solid, Mesomorphous Material. *Macromolecules* **1994**, *27*, 6007–6011.
26. Huang, M.; Schilde, U.; Kumke, M.; Antonietti, M.; Colfen, H. Polymer-Induced Self-Assembly of Small Organic Molecules into Ultralong Microbelts with Electronic Conductivity. *J. Am. Chem. Soc.* **2010**, *132*, 3700–3707.
27. Xie, M. Q.; Che, Y. X.; Liu, K.; Jiang, L. X.; Xu, L. M.; Xue, R. R.; Drechsler, M.; Huang, J. B.; Tang, B. Z.; Yan, Y. Caking-Inspired Cold Sintering of Plastic Supramolecular Films as Multifunctional Platforms. *Adv. Funct. Mater.* **2018**, *28*, 1803370.
28. Wu, L.; Willis, J. J.; McKay, I. S.; Diroll, B. T.; Qin, J.; Cargnello, M.; Tassone, C. J. High-Temperature Crystallization of Nanocrystals into Three-Dimensional Superlattices. *Nature* **2017**, *548*, 197.
29. Ober, C. K.; Wegner, G. Polyelectrolyte-Surfactant Complexes in the Solid State: Facile Building Blocks for Self-Organizing Materials.*Adv. Mater.* **1997**, *9*, 17–31.
30. Guillot, S.; Chemelli, A.; Bhattacharyya, S.; Warmont, F.; Glatter, O. Ordered Structures in Carboxymethylcellulose-Cationic Surfactants-Copper Ions Precipitated Phases: in Situ Formation of Copper Nanoparticles. *J. Phys. Chem. B.* **2009**, *113*, 15–23.
31. Martin, N.; Sharma, K. P.; Harniman, R. L.; Richardson, R. M.; Hutchings, R. J.; Alibhai, D.; Li, M.; Mann, S. Light-Induced Dynamic Shaping and Self-Division of Multipodal Polyelectrolyte-Surfactant Microarchitectures Via Azobenzene Photomechanics. *Sci. Rep.-UK* **2017**, *7*, 41327.
32. Koga, S.; Mann, S. Mesostructured Silica Hybrids from Liquid Polyelectrolyte-Surfactant-Aminosilanol Complexes. *J. Mater. Chem.* **2010**, *20*, 5736–5741.
33. Yeh, F. J.; Sokolov, E. L.; Khokhlov, A. R.; Chu, B. Nanoscale Supramolecular Structures in the Gels of Poly (diallyldimethylammonium chloride) Interacting with Sodium Dodecyl Sulfate. *J. Am. Chem. Soc.* **1996**, *118*, 6615–6618.
34. Zhou, S. Q.; Yeh, F. J.; Burger, C.; Chu, B. Nanostructures of Polyelectrolyte Gel-Surfactant Complexes. *J. Polym. Sci. Pol. Phys.* **1999**, *37*, 2165–2172.
35. Zhou, S. Q.; Burger, C.; Yeh, F. J.; Chu, B. Charge Density Effect of Polyelectrolyte Chains on the Nanostructures of Polyelectrolyte-Surfactant Complexes. *Macromolecules* **1998**, *31*, 8157–8163.
36. Winkler, U. K.; Stuckmann, M. Glycogen, Hyaluronate and Some Other Polysaccharides Greatly Enhance the Formation of Exolipase by Serratia Marcescens. *J. Bacteriol.* **1979**, *138*, 663–670.
37. Shi, J.; Deng, Q. C.; Li, Y.; Zheng, Z.; Shangguan, H. J.; Li, L.; Huang, F. H.; Tang, B. Homogeneous Probing of Lipase and α-amylase Simultaneously by AIEgens.*Chem. Commun.* **2019**, *55*, 6417–6420.

DOI: 10.31635/ccschem.020.201900088
CCS Chem. **2020**, *2*, 98–106